



Probing PARP1-inhibitor complexes for the development of novel inhibitors

U. Saqib¹ and M. S. Baig²*

¹ Maulana Azad National Institute of Technology (MANIT), Department of Mathematics, Kolar Road, Bhopal, Madhya Pradesh, 462007, India

² University of Illinois at Chicago (UIC), Department of Medicine, 909, South Wolcott Avenue, Chicago, IL-60612, USA

Corresponding author: Mirza Saqib Baig, University of Illinois at Chicago (UIC), Department of Medicine 909 South Wolcott Avenue, Chicago, IL-60612, USA. Tel: +312-622-7371, Fax: +507- 255-6318, Email: msb.uicmed@gmail.com

Abstract

Poly (ADP-ribose) polymerase 1 (PARP1) is the most important member of the PARP family which has been shown to have a direct involvement in the development of cancer. A strategy to rationalize the structure based drug discovery of PARP1 inhibitors has been discussed. So far studies regarding varied scaffold PARP1 inhibitors have been done, however the current study focus on how the available data from potent PARP1 inhibitors could be combined and utilized for developing a robust model for the development of novel inhibitors. Through detailed analyses of PARP1-inhibitor binding, a pharmacophore model has been developed followed by a virtual screen of potential inhibitors. The resulting high-affinity binding hits following the defined pharmacophore model and making the critical interactions were selected as final potential leads. Hence, using the approaches of pharmacophore design, docking based virtual screening and conformation alignment, we have identified important leads which satisfy all parameters of the screening process. The developed pharmacophore model as well as the strategy is very straightforward for screening novel inhibitors and could thus be used as a prototype for PARP1 structure based drug discovery.

Key words: PARP1, pharmacophore, virtual screening, docking, cancer.

Introduction

PARPs are cellular enzymes which catalyze the cleavage of its substrate NAD⁺ and transfer the ADP-ribose units to a number of acceptor proteins besides releasing the nicotinamide moiety (1). Among the 18 PARP family members, PARP-1 is the most commonly found and characterized member implicated in cellular responses to DNA injury due to genotoxic stress (2). PARP-1 plays an essential role in the repair of DNA single-strand breaks via the base excision repair pathway (3). It is a major component of a number of transcription factors involved in tumour development and inflammation (4-6). Rapid activation of PARP1 in response to alkylating-agent induced DNA strand breaks leads to resealing of DNA lesions (7). Hence, PARP1 activation induces various cell death processes thereby promoting an inflammatory response leading to multiple organ failure (8-11). The ever compelling evidence showing the direct role of PARP1 in the cellular response to genotoxic stress has led investigators to explore the result of PARP1 inhibition both for determining PARP1 function and therapeutic usage.

Structurally, PARP1 comprises three major domains including a DNA binding region which identify DNA strand breaks followed by a central automodification region and a third NAD binding region having the catalytic activity (12). PARP1 catalyzes the cleavage of NAD⁺ into ADP-ribose and further attaches several molecules of the latter to the target protein in a process called poly (ADP-ribosylation). Since NAD binding domain is responsible for PARP1 activity, many compounds mimicking the nicotinamide moiety of NAD were developed as PARP1 inhibitors (13-15). The discovery of PARP1 inhibitors goes back to more than three decades, where compounds based on substituted nicotinamide and ben-

zamide moieties were developed as competitive inhibitors of PARP1 (16). However, it was soon realized that such inhibitors lacked specificity and were rather affecting many other cellular processes like glucose metabolism, DNA synthesis etc (17). This was followed by a boom of benzamine analog inhibitors, which though shown to be highly specific, however were required in micromolar range (18). Benzamidazoles and their analogs have also been further developed and some others are even under various phases of clinical trials (19-24). However the major drawback associated with so far developed inhibitors is the frequent dosage required for them to be effective due to their low half-life (25).

All these factors drove us towards defining a well-defined model based on interaction mapping of potent and diverse inhibitors with PARP1 itself. In this strategy, we first identified the key interactions between PARP1 and its bound inhibitors in four different ligand-receptor complexes. Next, we identified the critical interactions common to all the four complexes. Based on the information by this interaction mapping, we derived a pharmacophore model, which encompass features and constraints which these four complexes had in common. Next, we docked two different ZINC databases having millions of compounds against PARP1. Further, we analysed the top 500 hits from each database retrieved after docking. We manually analysed each hit for binding site conformational superimposition with a high affinity PARP1 inhibitor, fitting with the developed pharmacophore model and finally retention of the critical receptor interactions. The resulting leads were diverse in their scaffolds and present a starting point for further evaluation as anti-PARP1 inhibitors. A flow diagram outlining the strategies employed in this study has been included in Fig.1.

Our study is the first showing a robust drug design

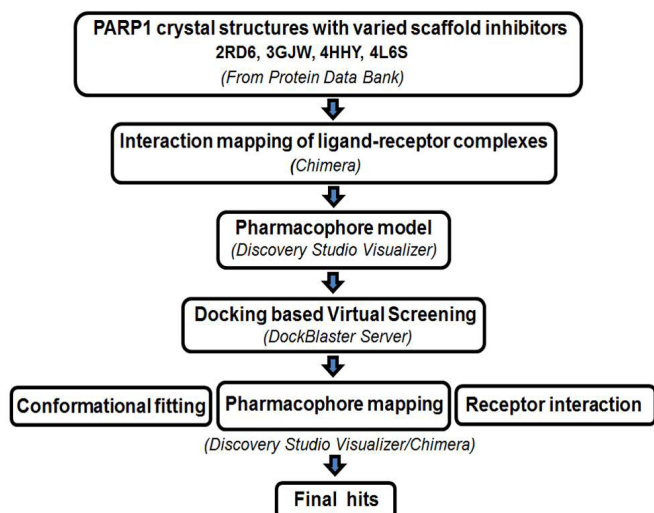


Figure 1. Flow diagram outlining the strategy employed in this work. Software resources and tools utilized are outlined in parentheses.

strategy for PARP1. To our knowledge, this is the first time a pharmacophore model based on binding of varied scaffold inhibitors with PARP1 has been developed. The final leads could further be evaluated as potential anti-PARP1 agents. We are sure that using our strategy any number of compounds could be easily and quickly screened *in-silico*. The developed pharmacophore model could be applied for any PARP1 inhibitor discovery with maximum accuracy. Thus our study will further lead to discovery and design of more potent PARP1 inhibitors.

Materials and methods

Interaction mapping of the receptor-ligand complexes

The co-crystal structures of PARP1 with four structurally diverse inhibitors (2RD6, 3GJW, 3L3L and 4HHY) (26-28) were retrieved from the Protein data bank. UCSF Chimera (29) was used for both visualization and analysis of the ligand-receptor complexes. We manually observed the overall interactions made by the respective inhibitor with the PARP1 binding site residues. Based on these observations we listed all those interactions which were common in all these four complexes.

Development of the pharmacophore model

Choosing and selecting the critical chemical feature is one of the most important steps in generating a pharmacophore. Features such as hydrogen-bond donor (HBD), ring-aromatic (RA), hydrogen-bond acceptor (HBA), were chosen based on individual assessment of the receptor-inhibitor complexes. Since all the four complexes consisted of structurally diverse scaffolds, we expected them to be variable in their interaction features. However, surprisingly after a thorough investigation of each of the complexes, we realized that all of them revolve around the same pharmacophore features. Therefore, the resulting pharmacophore model has been derived based on the consistency of the ligand-receptor interactions in all the four complexes. In other words, we identified the conserved features of the receptor-ligand complexes between the diverse scaffold inhibitors and PARP1. This could be further elaborated by taking the example of the donor amino group of the inhibitors which donates its

hydrogen to Gly202, or the aromatic ring which makes the stacking interactions with Tyr235, Tyr246. Similarly other interactions mapped were also consistent in all the four complexes. Further the constraints specified in the pharmacophore model too were adopted by averaging the respective distances in the individual complexes. For eg, the range of distance between the donor -amino (-NH₂) group and acceptor carboxy oxygen (=O) is between 2.2 Å and 2.4 Å, ring aromatic and donor amino group is between 2.8 Å and 3.7 Å, ring aromatic and acceptor oxygen is between 3.7 Å and 4.9 Å. We therefore assigned the average values of these distances between the various features of the pharmacophore model along with putting some flexibility to go higher and lower in range depending on the respective higher and lower values in all the four complexes. Discovery Studio Visualizer 4.0 (30) was utilized for manually identifying the various features of the resulting pharmacophore model.

Validation of the pharmacophore model

Further, the quality of the developed pharmacophore model has been confirmed by generating the Enrichment Factor (EF) and Goodness of Hit Score (GH) values. To verify the reliability of our developed pharmacophore model we used test set and decoy set validation. We collected 58 active compounds from the literature and constructed a three-dimensional database to be used as the test set. Further, we prepared a decoy set of compounds randomly from various databases which included 1822 molecules with unknown activity along with 18 active compounds. Enrichment Factor (EF) and Goodness of Hit Score (GH) were calculated to evaluate the model. EF and GH were calculated using below equations:

$$EF = (Ha / Ht) / (A / D)$$

$$GH = \{ [Ha * (3A + Ht)] / (4HtA) \} * [1 - (Ht - Ha) / (D - A)]$$

Where Ht is the number of hits retrieved, Ha is the number of active molecules in the hit list, A represents the number of active molecules present in the database and D stands for the total number of molecules in the decoy set. The GH score ranges from 0, indicating a null model to 1, which indicates an ideal model. When GH score is higher than 0.7, the model is considered to be good. Similarly a high EF indicates a superior model quality.

Virtual screening of compounds

Virtual screening technique has been used in drug discovery to search libraries of small molecules in order to identify those structures which are most likely to bind to a drug target (31-38). The docking calculations based on virtual screening were performed employing the DOCK Blaster server (39). Dock Blaster is a service for running docking screens and scores thousands of compounds deposited in the ZINC database (40) for a target structure uploaded by the user. The docking program used is DOCK 3.5.54 (41-44), a version of UCSF DOCK. DOCK Blaster pipeline is composed of six modules: (a) the parser, which identifies the receptor and ligand from a PDB file, (b) the scrutinizer, which attempts to correct for problems, such as incomplete or disordered residues on the receptor, (c) the preparer, which protonates the receptor, calculates "hot spots" and scoring grids, assigns atomic parameters, including

these for cofactors, post-translational modifications and metals, and prepares the ligand, decoys, and any actives and inactives for docking, (d) the calibrator, which uses supplied data to assess docking performance and suggests optimal docking parameters, (e) the docker, which manages a full database screen on the computer cluster, and (f) the assessor, which prepares reports to interpret database screening results. Two scoring schemes called “polarized” and “normal” are also used. The “normal” scheme uses standard AMBER 94 partial atomic charges on the protein, while “polarized” increases the dipoles on selected polar atoms in residues within 3.5Å of the crystallographic ligand without changing the net charge.

We used the crystal structure of PARP1 (2RD6) as receptor input and its bound inhibitor (78P) as the bound ligand for putative active site determination. After a few iterations for binding site determination, it returns few highly probable binding sites. Based on the available information, the user identifies one or more binding site for docking studies. Since, in our case, we already had a prior idea of the binding site based on the bound ligand, we selected the binding *site 1.1* given by the program. *Site 1.1* comprised all the critical residues we identified during interaction mapping. Further, we selected the ZINC subset 11 containing 5735035 entries as well as ZINC subset 12 containing 148310 entries. Compounds belonging to the former subset are more fragment like while the latter ones are described as lead-like and were selected to obey to the Lipinski rule, published in many reports (45-46). The docking parameters in Dockblaster comprise of preparation of the receptor which must be in PDB or mol2 format. A docked ligand in mol2 format (e.g. a crystallographically observed or modeled ligand) or a binding site specification in PDB format, which may be “hot spots” or atoms of binding site residues. The resulting 500 high-scoring hits from each database were eventually selected and analysed.

Analyses of hits

The high scoring hits were checked for (1) *conformational fitting*: based on superimposition with the bound inhibitor (2) *pharmacophore mapping*: manually fitted on the pharmacophore model in order to check that all constraints are obeyed (3) *presence of critical receptor interactions*: checked whether all major critical interactions suggested by the pharmacophore model are present. Only those hits were retained which followed all the three parameters. Hits which were either partially following the pharmacophore features or following only two of the three above parameters were also eliminated.

Results

Interaction mapping of the receptor-ligand complexes

Interaction mapping here stands for in-depth analysis of each of the four receptor-ligand complexes. Here we list all interactions made by the inhibitor with PARP1. Since, polar and non-polar interactions both play an important role in high binding affinity of the inhibitor to the receptor; we list all those interactions with respect to donor, acceptor, hydrophobic, aromatic groups etc, and eventually relate them with inhibitor binding. Below, we have discussed the interaction map of each of

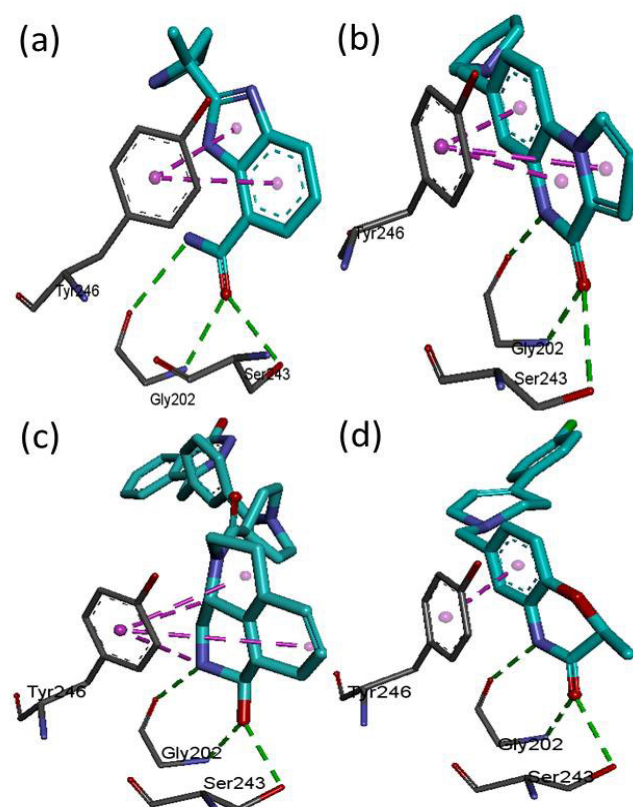


Figure 2. Interaction mapping of various PARP1- inhibitor complexes. For picture clarity only the critical residues are shown. PARP1 residues are shown as grey atom color and inhibitors as cyan atom color. The dashed magenta lines indicate hydrophobic pi-pi interactions, while the dashed green lines indicate hydrogen-bond (H-bond) interactions. Interaction analysis of (a) 2RD6 with A861695 (b) 3GJW with A968427 (c) 4HHY with 15R and (d) 4L6S with 1WQ shows the consistent polar interactions of the inhibitors with Gly202 and Ser243 and pi-pi interactions between the aromatic rings of inhibitors with the aromatic ring of Tyr246.

the four receptor-ligand complexes we used in the study.

2RD6:

The interaction between PARP1 and a high potency benzimidazol based inhibitor (A861695) was analysed (Fig. 2a). It was observed that the carbamoyl moiety was making two major polar interactions, where the oxy group (=O) was acting as H-bond acceptor by making a H-bond with the side chain hydroxyl (-OH) of Ser 243 and main chain amino (-NH₂) group of Gly 202. On the other hand, the -NH₂ group of the carbamoyl moiety is acting as a H-bond donor by donating a hydrogen to the main chain oxygen (=O) of carboxyl group of Gly 202, which thus acts as a H-bond acceptor. The benzimidazole ring is in turn making strong hydrophobic interactions with Lys 242, Tyr235, Tyr 228, Phe 236, and Trp 200, besides making a closer pi-pi stacking interaction with Tyr 246. Here we observe that the presence of a donor and an acceptor group or specifically a carbamoyl group in the vicinity of Gly202 and Ser243 and the presence of a phenyl/aromatic ring in the vicinity of Tyr235, Tyr246 and other hydrophobic residues is important for the ligand binding.

3GJW:

The interaction between PARP1 and a quinoxalinone-based inhibitor (A968427) was analysed (Fig. 2b). The -NH of the Quinoxalinone ring is acting as a

H-bond donor by donating a hydrogen to the main chain =O of carboxyl group of Gly202. Further, the =O of the Quinoxalinone ring is acting as an acceptor for both side chain -OH group of Ser243 and main chain -NH₂ group of Gly202. At the same time, the Quinoxalinone ring itself is important for pi-pi interactions with Tyr235, Tyr246, His201 and other hydrophobic interactions with Ala237 and Lys242 etc. Same as in 2RD6, the presence of donor, acceptor groups in the vicinity of Gly202 and Ser243 and an aromatic ring near Tyr235, Tyr246 etc seem to be important for inhibitor binding.

4HHY:

The interaction between PARP1 and benzonaphthyridinone based inhibitor (15R) was analysed (Fig. 2c). The -NH and =O of piperidinone ring make H-bond interactions with the side chain -OH of Ser243 and main chain -NH of Gly202 as discussed for 2RD6. At the same time the benzene ring next to the piperidinone ring is making hydrophobic interactions with Leu108, Arg217, His201 etc and pi-pi stack interactions with Tyr235 and Tyr246. Here again, the presence of hydrogen donor -NH and acceptor =O near Ser243 and Gly243 along with an aromatic ring near Tyr235, Tyr246, His201 etc seems to be important for inhibitor binding.

4L6S:

PARP1 binding with benzoxazinone based inhibitor (1WQ) was analyzed (Fig.2d). The =O and -NH of the benzoxazinone ring makes the usual Ser243 and Gly202 polar interactions as present in other complexes discussed above. While the benzene ring of the benzoxazinone makes similar hydrophobic interactions with Tyr235, His201, Asp105, Asn106, Leu108, Arg217 and pi-pi stack interaction with Tyr246.

The common features were individually extracted from all the four receptor-ligand complexes (Fig3a-3d).

Development of the pharmacophore model

The pharmacophore model was developed with an intention to characterize all the common interactions involved between varied inhibitors and PARP1. After a thorough investigation, we concluded that the polar interactions between the (1) side chain hydroxyl (-OH) of Ser 243 and the inhibitor acceptor group (=O) (2) main chain amino (-NH₂) group of Gly 202 and inhibitor acceptor group (=O) (3) main chain carboxyl oxygen (=O) of Gly 202 and the amino (-NH₂) group of inhibitor ; and pi-pi interactions between (4) the ring of Tyr 246 and aromatic ring of the inhibitor are common in all four complexes. Another point to be noted here is that besides the critical interactions we discussed above, there were few “accessory” interactions present, like the polar and non-polar interactions between ligand groups and His 201, Lys 242, Ala 237, Tyr 235. However, we did not add these in the final pharmacophore model, due to the absence of either of these interactions in any of the four complexes. As mentioned earlier, this is due to the reason that we wanted to incorporate only those features in the pharmacophore model which were common in all the four complexes. The derived pharmacophore model hence consisted of: one acceptor feature which act as a H-bond acceptor for Ser 243 and Gly 202, one donor feature which act as a H-bond donor for Gly 202, and at least one aromatic ring near the vicinity of Tyr 246 for the highly important and conserved pi-pi stacking interaction. After a deep and careful analysis of each of the four receptor-ligand complexes, we also made an interesting finding that the distances between the various pharmacophore features discussed above are also conserved as discussed in the Methods sections. Assigning distance constrains had an added advantage to our model, as only features in a pharmacophore model could lead to unreasonably large number of hits if the latter is

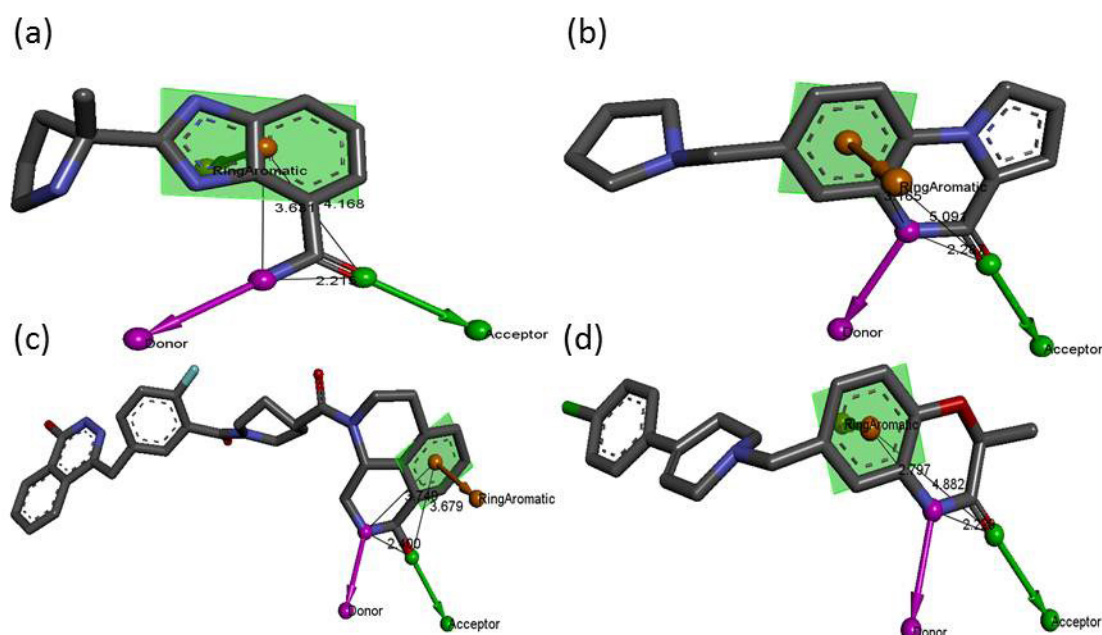


Figure 3. Common feature derivation by interaction mapping of the PARP1-inhibitor complexes. Inhibitors are colored as grey atom color, the donor features as magenta balls and arrows, acceptor features as green balls and arrows while the aromatic ring as orange ball and green squares. Black lines indicate the distance between various features. (a) A861695 has -NH₂ group acting as a H-donor and =O group acting as a H-acceptor, while the benzimidazole ring is making an aromatic centroid for stacking interactions (b) A968427 has -NH₂ group and =O group as H-bond donor and acceptor respectively and Quinoxalinone ring for putative pi-pi stacking interactions (c) 15R has -NH and =O for H-bond interactions and the piperidinone ring for hydrophobic interactions (d) 1WQ has the =O and -NH groups as H-bond acceptor and donor respectively while the benzene ring for hydrophobic pi-pi interactions.

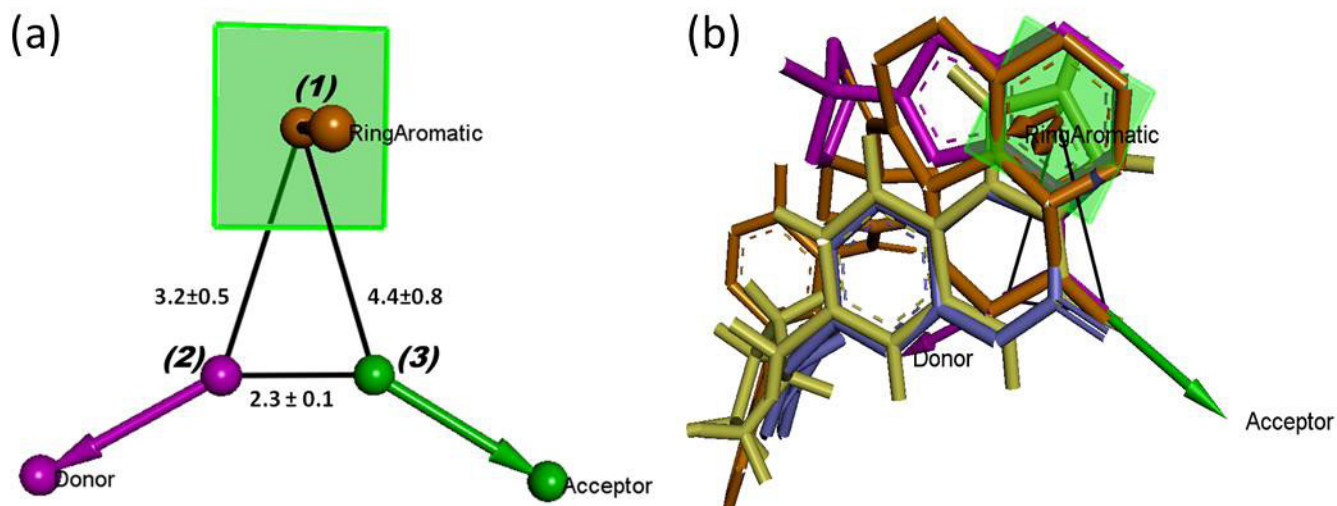


Figure 4. (a) Pharmacophore model derived after interaction mapping of the PARP1-inhibitor complexes. It encompasses a donor group (magenta ball and arrow), an acceptor group (green ball and arrow) and a ring aromatic centroid (orange ball and green square). The distance constraints between various pharmacophore features has been shown as black solid lines, (b) mapping of all four inhibitors onto the pharmacophore model, where A861695 is colored in magenta, A968427 in light yellow, 15R in orange and 1WQ in light blue.

used for a virtual screen, however due to constraints in the model comparatively lower number of hits would be retrieved. This reduces the time for short-listing any virtual screen library and hence very specific hits could be shortlisted in relatively shorter time. Figure 4 illustrates the derived pharmacophore model along with mapping of all four inhibitors on it.

Validation of the pharmacophore model

58 active compounds from the literature were docked and mapped onto the pharmacophore model to check the number of features superimposing with the model (data not shown). As we expected most of the compounds aligned very well with the pharmacophore model. However very few compounds failed to follow the pharmacophore model in the distance constraint aspect, which is understandable, as the distances do vary in hydrogen-bond and ring-ring interactions and therefore cannot exactly follow the stringency of the model. Hence, the result of the test set validation confirmed the ability of our pharmacophore model to retrieve active hits. However, since this result could only indicate that our pharmacophore model can pick out the active molecules, we moved on to check its ability to exclude compounds without inhibitory activity (decoys). The main reason to validate the pharmacophore by decoy set is to validate how well it predicts active molecules from inactive molecules. From a decoy set of 1822 random compounds with unknown activity and 18 active compound from the literature, we performed further pharmacophore validation where, 14 active compounds and 6 molecules with unknown activity were retrieved. The EF and GH were calculated to be 71.4 and 0.72 respectively thus indicating that the developed pharmacophore model is reliable for any virtual screening protocol.

Virtual screening and analyses of compounds

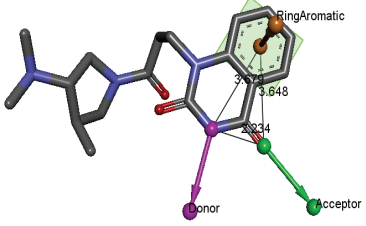
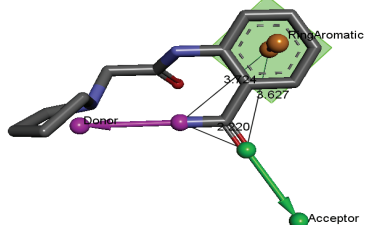
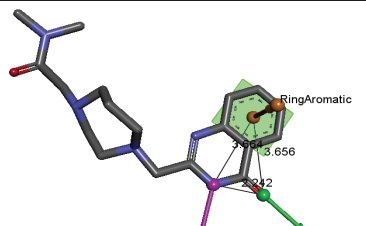
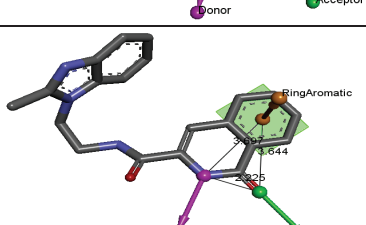
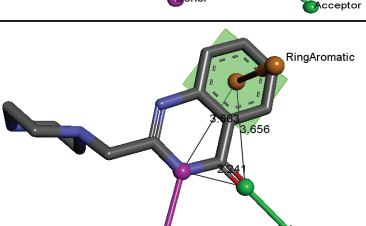
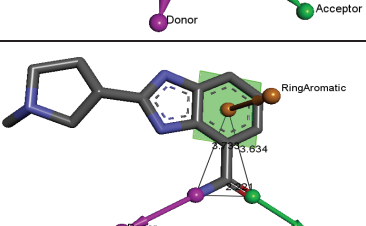
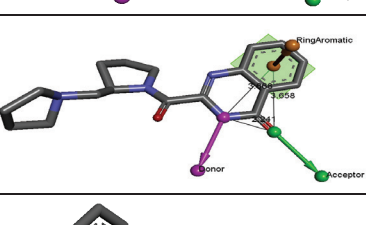
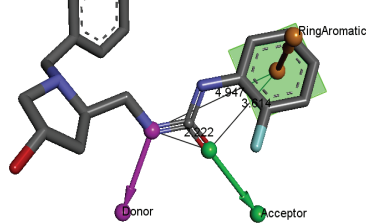
Further, we ran a docking based virtual screen for novel PARP1 inhibitors using the Dock blaster program. Two different databases, clean leads #11 (5735035 compounds), and clean fragments #12 (148310) were used in order to screen inhibitors with diverse scaffolds. The resulting top high-scoring 500 hits from each database

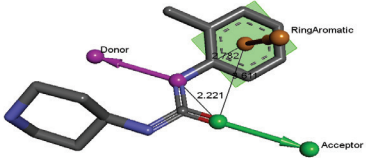
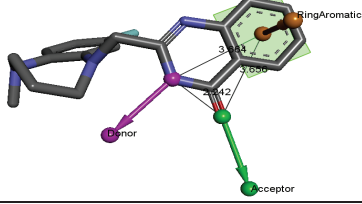
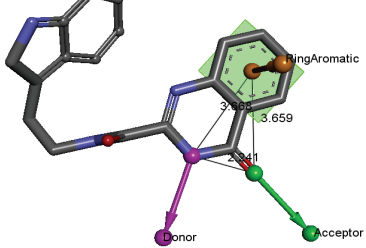
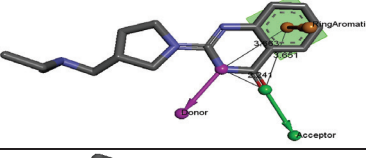
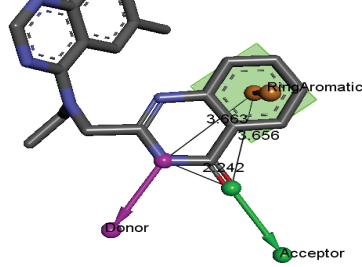
were then manually analysed. We tried to identify hits which follow all three parameters of screening including (1) conformational fitting (2) pharmacophore model fitting and (3) fulfilment of the critical interactions. Out of the top 500 hits from each database, nearly 55 hits were perfectly following the screening criteria. These hits were not only superimposable with the binding conformation of one of the most potent PARP1 inhibitor A861695 (2RD6), but as expected were also mimicking the required receptor interactions made by A861695 along with fitting very well with the pharmacophore model. **Table 1** with few of the top hits shows how well they fit in the pharmacophore model. All the hits bind at the same place in PARP1 binding site (Fig 5). As clearly observed in the figure, all the top screened hits are superimposing perfectly with the conformation of the bound inhibitor (A861695). The docked conformations of few of the high binding compounds or 'hits' are shown in Fig 6. For clarity reasons A861695 is not shown alongside the docked hits. However, Fig.5 clearly shows how well they superimpose with each other. Compound AAZ (Fig 6a), besides perfectly superimposing with the bound conformation of co-crystallized ligand in the PARP1 binding site and following the pharmacophore model, makes all the critical interactions like those with Ser 243, Gly 202 and Tyr 246. The -NH and =O of Quinoxalinone ring makes interactions very similar to that made by inhibitor A968427 (discussed above). The carbamoyl moiety and the phenyl ring of ABE (Fig 6b) makes interactions similar to inhibitor A861695. The benzimidazole and the carbamoyl moieties of AES (Fig 6c) and the carbamoyl substituted phenyl ring of AGJ (Fig 6d) also follow the above discussed trend. Compounds AAZ, ABE, AES and AGJ could also be observed fitting perfectly with the pharmacophore model in Table 1.

Discussion

The continuous development and further improvement of target specific inhibitors is of considerable importance to any drug discovery project. However, inspite of discovery of many diverse and highly potent

Table 1. Structures of top hits fitted on the pharmacophore model shown with their Dock blaster binding energies.

Zinc Library	Compound Name	Structure	Binding energy (kcal/mol)
clean leads #11	AAZ		-60.67
clean fragments #12	ABE		-49.13
clean leads #11	ACJ		-58.89
clean leads #11	ADI		-58.22
clean fragments #12	ADU		-47.59
clean fragments #12	AES		-47.19
clean leads #11	AEW		-57.57
clean leads #11	AGJ		-57.08

clean fragments #12	AHW		-46.37
clean leads #11	AJK		-56.63
clean leads #11	AKE		-56.51
clean leads #11	AMK		-56.24
clean leads #11	AQM		-55.84

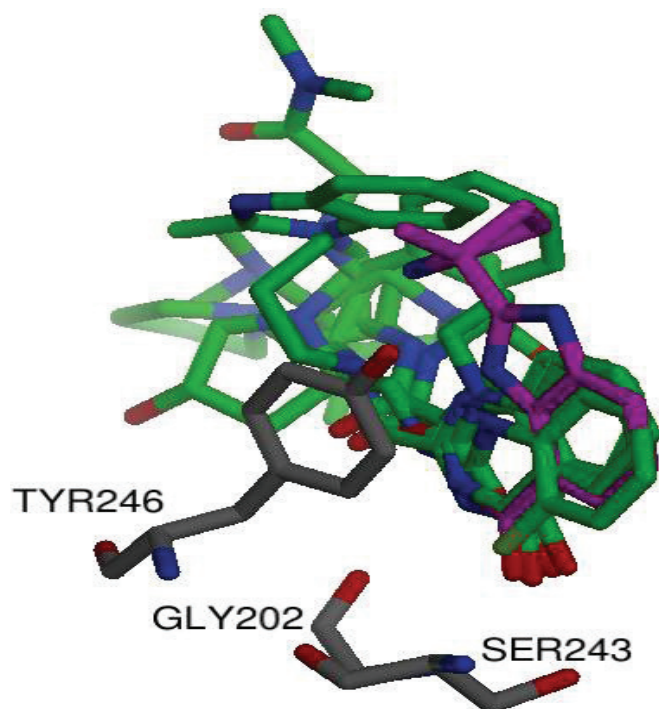


Figure 5. Superimposition of hits with A861695 in the PARP1 binding site. PARP1 residues are shown as grey atom color, A861695 is shown as magenta atom color and few of the top hits are shown as green atom color. The hits align perfectly with the crucial polar and non-polar features of the bound inhibitor (A861695).

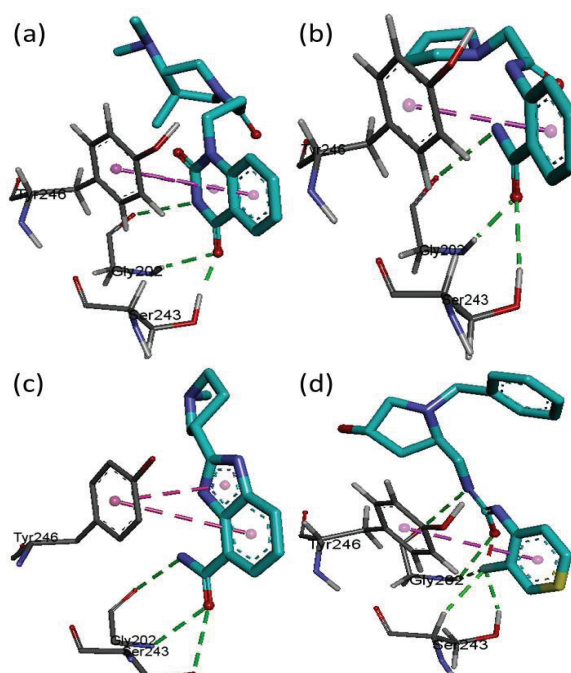


Figure 6. Docked poses of top scoring hits in the binding site of PARP1. PARP1 residues are shown as grey atom color, while the hits are shown in cyan atom color. H-bond interactions are shown as green dashed lines and the pi-pi interactions are shown as the magenta dashed lines. Compound (a) AAZ (b) ABE (c) AES (d) AGJ bind to the PARP1 binding site as described in the text, making the crucial H-bond and pi-pi interactions.

inhibitors, there is a lack of structural guidelines which can establish key features in the inhibitors responsible for their activity. If we take the example of Protein Tyrosine Phosphatase 1B (PTP1B), a very important target for type 2 diabetes and study the latest literature about its structure based drug design, we will realize that how much efforts investigators have put to crack down the structural features responsible for the inhibitor activity. This development includes, developing fingerprints, pharmacophore models, and other strategies which would help future PTP1B drug discovery efforts easier. These efforts have completely sidelined the trivial and old fashioned drug discovery programs where the investigators either start from scratch in order to develop a totally new inhibitor or modify the existing high-potency inhibitor in order to make a better candidate. We had the same concern for PARP1, as it has been shown to be a very important target for many diseases including cancer, inflammation etc. We realized that in spite of potent and diverse scaffold inhibitors, there are no proper analyses of the regions and features responsible for the high binding affinity between the target and inhibitor. Hence, we started our study with an intention to develop a pharmacophore model, which would be complete in itself in determining the efficacy or binding affinity of any new compound for PARP1. In the present study, four varied scaffold inhibitors bound to the PARP1 crystal structure were used to develop a pharmacophore model. These inhibitors belong to diverse scaffolds like benzimidazol, quinoxalinone, benzooxazinone and benzonaphthyridinone. Though we also analysed various other PARP1-inhibitor complexes, but since all of them fell into one the above mentioned categories, therefore we took a representative from each. Next, we deeply examined each of these PARP1-inhibitor complexes. Each complex was first analyzed for the binding interactions between the co-crystallized inhibitor and PARP1. After mapping the interaction pattern of each of these four structures, we listed all the polar and non-polar interactions present between respective receptor-ligand complexes. Then we checked for those interactions which were common to all four complexes and eventually came up with a pharmacophore model which encompasses all the critical features of PARP1 inhibitors responsible for high activity. Further, we also added distance constraints between the features, as we realized that distance between various pharmacophore features is more or less conserved in all receptor-ligand complexes. This is also true for complexes besides the four we used in the study (data not shown). The motto of developing the pharmacophore model was not just to develop a screening system for potential PARP1 inhibitors, but also to develop a universal model which could be used as a prototype for future PARP1 inhibitor drug discovery. Further, validation of the pharmacophore model also reveals the superior quality of the developed model with high Enrichment Factor (EF) and Goodness of Hit Score (GH) values of 71.4 and 0.72 respectively. Next, ZINC libraries with millions of compounds were docked against PARP1 receptor in order to retrieve potential hits. Each ZINC library available in the Dock blaster program contains millions of diverse scaffold compounds and in order to increase the diversity we took both fragment-based and lead-based

libraries. Finally, the high-scoring hits from each of the libraries were individually analyzed for their conformational fitting against a known high-affinity PARP1 inhibitor A861695 (2RD6), fitting on the pharmacophore model and interaction with PARP1. Only those hits which completely fulfilled the three screenings were eventually selected as final leads. After a closer look at the final leads, it was found that these leads belong to various scaffolds like quinoxal, quinazoline, benzimidazole, pyrrolidine, triazol and many more. They fit in the PARP1 binding site at exactly the same place as other high-affinity PARP1 inhibitors. Thus novel leads are discovered from this study, which though mimic the high affinity PARP1 inhibitors, but lack the drawbacks of the already available inhibitors by being diverse in their nature. These could further be advanced for various assays in order to check for potency in vitro. Finally, this is the first study where a pharmacophore model has been developed based on varied scaffold inhibitors which could be universally applied in order to screen novel PARP1 inhibitors.

Acknowledgements

We thank the team at the Department of Mathematics, MANIT for providing facilities for performing *insilico* studies. We also thank Dr. Appu Kuttan KK, Director MANIT for all the encouragement and help he provided us during this project.

References

1. Chambon, P., Weill, J.D. and Mandel, P., Nicotinamide mononucleotide activation of new DNA-dependent polyadenylic acid synthesizing nuclear enzyme. *Biochem. Biophys. Res. Commun.* 1963, **11**: 39-43. doi: 10.1016/0006-291X(63)90024-X.
2. Jagtap, P. and Szabó, C., Poly (ADP-ribose) polymerase and the therapeutic effects of its inhibitors. *Nat. Rev. Drug Disc.* 2005, **4**: 421-440. doi: 10.1038/nrd1718.
3. D'Amours, D., Desnoyers, S., D'Silva, I. and Poirier, G.G., Poly (ADP-ribosyl)ation reactions in the regulation of nuclear functions. *Biochem. J.* 1999, **342**: 249-268. doi: 10.1042/0264-6021:3420249.
4. Oliver, F.J., Ménissier-de Murcia, J., Nacci, C., Decker, P., Andriantsitohaina, R., Muller, S., de la Rubia, G., Stoclet, J.C., de Murcia, G., Resistance to endotoxic shock as a consequence of defective NF-kappaB activation in poly (ADP-ribose) polymerase-1 deficient mice. *EMBO J.* 1999, **18**:4446-4454. doi: 10.1093/emboj/18.16.4446.
5. Goyal, N., Duncan, R., Selvapandiyani, A., Debrabant, A., Baig, M.S., Nakhasi, H.L. Cloning and characterization of angiotensin converting enzyme related dipeptidylcarboxypeptidase from *Leishmania donovani*. *Mol. Biochem. Parasitol.* 2006, **145**(2):147-57. doi: 10.1016/j.molbiopara.2005.09.014.
6. Baig, M.S., Gangwar, S. and Goyal, N. Biochemical characterization of dipeptidylcarboxypeptidase of *Leishmania donovani*. *Cell. Mol. Biol. (Noisy-le-grand)* 2011, **57**(1):56-61.
7. Esteller, M., Garcia-Foncillas, J., Andion, E., Goodman, S.N., Hidalgo, O.F., Vanaclocha, V., Baylin, S.B. and Herman, J.G. Inactivation of the DNA-Repair Gene MGMT and the Clinical Response of Gliomas to Alkylating Agents. *The N. Engl. J. Med.* 2000, **343**:1350-1354. doi: 10.1056/NEJM200011093431901.
8. Hassa, P.O., Haenni, S.S., Elser, M. and Hottiger, M.O., Nuclear ADP-ribosylation reactions in mammalian cells: where are we today and where are we going? *Microbiol. Mol. Biol. Rev.* 2006, **70**:789-829. doi: 10.1128/MMBR.00040-05.

9. Haenni, S.S., Hassa, P.O., Altmeyer, M., Fey, M., Imhof, R., Hot-tiger, M.O., Identification of lysines 36 and 37 of PARP-2 as targets for acetylation and auto-ADP-ribosylation. *Int. J. Biochem. Cell. Biol.* 2008, **40**: 2274-2283. doi: 10.1016/j.biocel.2008.03.008.
10. Wang, Z.Q., Auer, B., Sting, L., Berghammer, H., Haidacher, D., Schweiger, M., Wagner, E.F., Mice lacking ADPRT and poly(ADP-ribosyl)ation develop normally but are susceptible to skin disease. *Genes Dev.* 1995, **9**:509-520. doi: 10.1101/gad.9.5.509.
11. Shall, S., and de Murcia, G., Poly(ADP-ribose) polymerase-1: what have we learned from the deficient mouse model? 2000, *Mutat Res.* **460**:1-15. doi: 10.1016/S0921-8777(00)00016-1.
12. Kurosaki, T., Ushiro, H., Mitsuchi, Y., Suzuki, S., Matsuda, M., Matsuda, Y. et al., Primary structure of human poly(ADP-ribose) synthetase as deduced from cDNA sequence. *J. Biol. Chem.* 1987, **262**:15990-15997.
13. Ruf, A., Mennissier de Murcia, J., de Murcia, G. and Schulz, G.E., Structure of the catalytic fragment of poly(AD-ribose) polymerase from chicken. *Proc. Natl. Acad. Sci.* 1996, **93**:7481-7485. doi: 10.1073/pnas.93.15.7481.
14. Ruf, A., de Murcia, G. and Schulz, G.E., Inhibitor and NAD⁺ binding to poly(ADP-ribose) polymerase as derived from crystal structures and homology modeling. *Biochemistry* 1998, **37**:3893-3900. doi: 10.1021/bi972383s.
15. Oliver, A.W., Ame, J.C., Roe, S.M., Good, V., de Murcia, G. and Pearl, L.H., Crystal structure of the catalytic fragment of murine poly(ADP-ribose) polymerase-2. *Nucleic Acids Res.* 2004, **32**:456-464. doi: 10.1093/nar/gkh215.
16. Purnell, M.R. and Wish, W.J., Novel inhibitors of poly(ADP-ribose) synthetase. *Biochem. J.* 1980, **185**:775-777.
17. Milam, K.M. and Cleaver, J.E., Inhibitors of poly(adenosine diphosphate-ribose) synthesis: effect on other metabolic processes. *Science* 1984, **223**:589-591. doi: 10.1126/science.6420886.
18. Banasik, M., Komura, H., Shimoyama, M. and Ueda, K., Specific inhibitors of poly(ADP-ribose) synthetase and mono(ADP-ribose)transferase. *J. Biol. Chem.* **267**:1569-1575.
19. Canan Koch, S.S., Thoresen, L.H., Tikhe, J.G., Maegley, K.A., Almasy, R.J., Li, J., Yu, X.H., Zook, S.E., Kumpf, R.A., Zhang, C., Boritzki, T.J., Mansour, R.N., Zhang, K.E., Ekker, A., Calabrese, C.R., Curtin, N.J., Kyle, S., Thomas, H.D., Wang, L.Z., Calvert, A.H., Golding, B.T., Griffin, R.J., Newell, D.R., Webber, S.E. and Hostomsky, Z., Novel tricyclic poly(ADP-ribose) polymerase-1 inhibitors with potent anticancer chemopotentiating activity: design, synthesis, and X-ray cocrystal structure. *J. Med. Chem.* 2002 **45**:4961-4974. doi: 10.1021/jm020259n.
20. Plummer, R., Jones, C., Middleton, M., Wilson, R., Evans, J., Olsen, A., Curtin, N., Boddy, A., McHugh, P., Newell, D., Harris, A., Johnson, P., Steinfeldt, H., Dewji, R., Wang, D., Robson, L. and Calvert, H., Phase I study of the poly(ADP-ribose) polymerase inhibitor, AG014699, in combination with temozolomide in patients with advanced solid tumors. *Cancer Res.* 2008, **14**:7917-7923. doi: 10.1158/1078-0432.CCR-08-1223.
21. Aoyagi-Scharber, M., Gardberg, A.S., Yip, B.K., Wang, B., Shen, Y. and Fitzpatrick, P.A., Structural basis for the inhibition of poly(ADP-ribose) polymerases 1 and 2 by BMN 673, a potent inhibitor derived from dihydropyridophthalazinone. *Acta Crystallographica Section F Structural Biology and Crystallization Communications.* 2014, **70(Pt 9)**:1143-1149. doi: 10.1107/S2053230X14015088.
22. Penning, T.D., Zhu, G.D., Gandhi, V.B., Gong, J., Liu, X., Shi, Y., Klinghofer, V., Johnson, E.F., Donawho, C.K., Frost, D.J., Bontcheva-Diaz, V., Bouska, J.J., Osterling, D.J., Olson, A.M., Marsh, K.C., Luo, Y. and Giranda, V.L., Discovery of the poly(ADP-ribose) polymerase (PARP) inhibitor 2-[(R)-2-methylpyrrolidin-2-yl]-1H-benzimidazole-4-carboxamide (ABT-888) for the treatment of cancer. *J. Med. Chem.* 2009, **52**:514-523. doi: 10.1021/jm801171j.
23. Huang, S.H., Xiong, M., Chen, X.P., Xiao, Z.Y., Zhao, Y.F. and Huang, Z.Y., PJ34, an inhibitor of PARP-1, suppresses cell growth and enhances the suppressive effects of cisplatin in liver cancer cells. *Oncol. Rep.* 2008, **20**: 567-572. doi: 10.3892/or_00000043.
24. Menear, K.A., Adcock, C., Boulter, R., Cockcroft, X.L., Copsey, L., Cranston, A., Dillon, K.J., Drzewiecki, J., Garman, S., Gomez, S., Javaid, H., Kerrigan, F., Knights, C., Lau, A., Loh, V.M. Jr., Matthews, I.T., Moore, S., O'Connor, M.J., Smith, G.C. and Martin, N.M., 4-[3-(4-Cyclopropanecarbonylpiperazine-1-carbonyl)-4-fluorobenzyl]-2H-phth alazin-1-one: a novel bioavailable inhibitor of poly(ADP-ribose) polymerase-1. *J. Med. Chem.* 2008, **51**:6581-6591.
25. Donawho, C. K., Luo, Y., Luo, Y., Penning, T.D., Bauch, J.L., Bouska, J.J. et al., ABT-888, an orally active poly(ADP-ribose) polymerase inhibitor that potentiates DNA-damaging agents in pre-clinical tumor models. *Clin. Cancer Res.* 2007, **13**:2728-2737. doi: 10.1158/1078-0432.CCR-06-3039.
26. Miyashiro, J., Woods, K.W., Park, C.H., Liu, X., Shi, Y., Johnson, E.F. et al., Synthesis and SAR of novel tricyclic quinoxalinone inhibitors of poly(ADP-ribose)polymerase-1 (PARP-1). *Bioorg. Med. Chem. Lett.* 2009, **19**: 4050-4054. doi: 10.1016/j.bmcl.2009.06.016.
27. Gandhi, V.B., Luo, Y., Liu, X., Shi, Y., Klinghofer, V., Johnson, E.F. et al., Discovery and SAR of substituted 3-oxoisindoline-4-carboxamides as potent inhibitors of poly(ADP-ribose) polymerase (PARP) for the treatment of cancer. *Bioorg. Med. Chem. Lett.* 2010, **20**:1023-1026. doi: 10.1016/j.bmcl.2009.12.042.
28. Ye, N., Chen, C.H., Chen, T., Song, Z., He, J.X., Huan, X.J. et al., Design, synthesis, and biological evaluation of a series of benzo[de][1,7]naphthyridin-7(8H)-ones bearing a functionalized longer chain appendage as novel PARP1 inhibitors. *J. Med. Chem.* 2013, **56**:2885-2903. doi: 10.1021/jm301825t.
29. Pettersen, E.F., Goddard, T.D., Huang, C.C., Couch, G.S., Greenblatt, D.M., Meng, E.C, et al., UCSF Chimera--a visualization system for exploratory research and analysis. *J. Comput. Chem.* 2004, **25**:1605-1612. doi: 10.1002/jcc.20084.
30. Accelrys Software Inc., Discovery Studio Modeling Environment, Release x.x , San Diego: Accelrys Software Inc., 2007.
31. Trane, A.E., Pavlov, D., Sharma, A., Saqib, U., Lau, K., van Petegem, F., Minshall, R.D., Roman, L.J., Bernatchez, P.N. Deciphering the binding of caveolin-1 to client protein endothelial nitric oxide synthase (eNOS): scaffolding sub-domain identification, interaction modeling, and biological significance. *The Journal of Biological Chemistry* 2014, **289(19)**:13273-13283. doi: 10.1074/jbc.M113.528695.
32. Saqib, U., Kumar, B. and Siddiqi, M.I. Structural Investigations of Anthranilimide Derivatives by CoMFA and CoMSIA 3D-QSAR Studies Reveal Novel Insight into Their Structures toward glycogen phosphorylase Inhibition. *SAR and QSAR in Environmental Research*, 2011, **22(5-6)**:411-449. doi: 10.1080/1062936X.2011.569898.
33. Saqib, U. and Siddiqi, M.I. 3D-QSAR studies of xanthone derivatives as human alpha glucosidase inhibitors. *International Journal of Integrative Biology.* 2009, **5**:13-19.
34. Saqib, U. and Siddiqi M.I. 3D-QSAR studies on triazolopiperazine amide inhibitors of dipeptidyl peptidase-IV as anti-diabetic agents. *SAR and QSAR in Environmental Research.* 2009, **20**:519-535. doi: 10.1080/10629360903278677.
35. Saqib, U. and Siddiqi, M.I. Probing ligand binding interactions of human alpha glucosidase by homology modeling and molecular docking. *Int. Journal of Integrative Biology.* 2008, **2 (2)**: 116-121.
36. Gupta, A., Mir, S.S., Saqib, U., Biswas, S., Vaishya, S., Srivastava, K., Siddiqi, M.I., Habib, S. The effect of fusidic acid on Plasmodium falciparum elongation factor G (EF-G). *Mol. Biochem. Parasitol.* 2013, **192(1-2)**:39-48. doi: 10.1016/j.molbiopara.2013.10.003.
37. Singh, M., Shrivastava, N., Saqib, U., Siddiqi, M.I. and Misra-

- Bhattacharya, S. Structural modelling studies and immunoprophylactic potential of *Brugia malayi* DEAD Box RNA helicase. *Parasitology*, 2013, **140**(8):1016-1025. doi: 10.1017/S0031182013000322.
38. Biswas, S., Lim, E.E., Gupta, A., Saqib, U., Mir, S.S., Siddiqi, M.I., Ralph, S.A. and Habib S. Interaction of apicoplast-encoded elongation factor (EF) EF-Tu with nuclear-encoded EF-Ts mediates translation in the *Plasmodium falciparum* plastid. *Int. J. Parasitol.* 2011, **41**:417-427. doi: 10.1016/j.ijpara.2010.11.003.
39. Irwin, J.J., Shoichet, B.K., Mysinger, M.M., Huang, N., Colizzi, F., Wassam, P. et al., Automated docking screens: a feasibility study. *J. Med. Chem.* 2009, **52**:5712-5720. doi: 10.1021/jm9006966.
40. Irwin, J.J., Sterling, T., Mysinger, M.M., Bolstad, E.S. and Coleman, R.G., ZINC: a free tool to discover chemistry for biology. *J. Chem. Inf. Model.* 2012, **52**: 1757–1768. doi: 10.1021/ci3001277.
41. Meng, E. C., Shoichet, B. K. and Kuntz, I. D., Automated docking with grid-based energy evaluation. *J. Comput. Chem.* 1992, **13**: 505-524. doi: 10.1002/jcc.540130412.
42. Shoichet, B.K. and Kuntz, I.D., Matching chemistry and shape in molecular docking. *Protein Engineering* 1993, **6**: 723-732. doi: 10.1093/protein/6.7.723.
43. Gangwar, S., Baig, M.S., Shah, P., Biswas, S., Batra, S., Siddiqi, M.I. and Goyal N. Identification of novel inhibitors of dipeptidyl-carboxypeptidase of *Leishmania donovani* via ligand-based virtual screening and biological evaluation. *Chem. Biol. Drug. Des.* 2012, **79**(2):149-156. doi: 10.1111/j.1747-0285.2011.01262.x.
44. Baig, M.S., Kumar, A., Siddiqi, M.I. and Goyal, N. Characterization of dipeptidylcarboxypeptidase of *Leishmania donovani*: a molecular model for structure based design of antileishmanials. *J. Comput. Aided Mol. Des.* 2010, **24**(1):77-87. doi: 10.1007/s10822-009-9315-y.
45. Baig, M.S. and Manickam, N. Homology modeling and docking studies of *Comamonas testosteroni* B-356 biphenyl-2,3-dioxygenase involved in degradation of polychlorinated biphenyls. *Int. J. Biol. Macromol.* 2010, **46**(1):47-53. doi: 10.1016/j.ijbiomac.2009.10.014.
46. Lipinski, C.A., Lombardo, F., Dominy, B.W. and Feeney, P.J. Experimental and computational approaches to estimate solubility and permeability in drug discovery and development settings. *Adv. Drug Delivery Rev.* 1997, **23**: 3–25. doi: 10.1016/S0169-409X(96)00423-1.